MIT Kavli Institute   Chandra X-Ray Center

1 Overview

It is widely known among *Chandra*/HETG spectroscopists that the background rate in HETG/ACIS dispersed spectra is very low. It is also known that the gratings greatly reduce the flaring background due to energetic particles.[1] However, there is little documentation on the background with the HETGS, aside from an early figure in the *Proposers' Observatory Guide* (or *POG*) (§8.2.3). While the information there (revisions Cycle 19 or before) is technically correct, it is an overestimate, since it is based on a very bright coronal source (HR 1099, V711 Tau, observation ID 62538). As such, there may be a significant contribution of source photons aliased in CCD `CHIPY` during the frame readout (since exposure continues during the frame-shift). Hence, it is time to revisit the HETG background and provide a more extensive analysis of what is generally taken for granted, since we have much more data in the archive upon which to draw.

Here we have used several HETG observations which were long and of faint or heavily absorbed sources (see Table 1). The latter are useful at long wavelengths since the source spectrum is highly attenuated on the outer array CCDs. We have extracted first order HETG spectra off-source, using small modifications to standard processing, the primary result is shown in Figure 1. The small spatial region of a resolution element (both along and perpendicular to the dispersion axis) coupled with CCD energy resolution ("PHA" filtering at the CCD resolution, used to sort spatially overlapping orders) strongly suppresses background counts.

---

[1] `https://arxiv.org/abs/astro-ph/0202086` Grant et al., 2002, "The temporal characteristics of the Chandra X-ray Observatory high energy particle background".
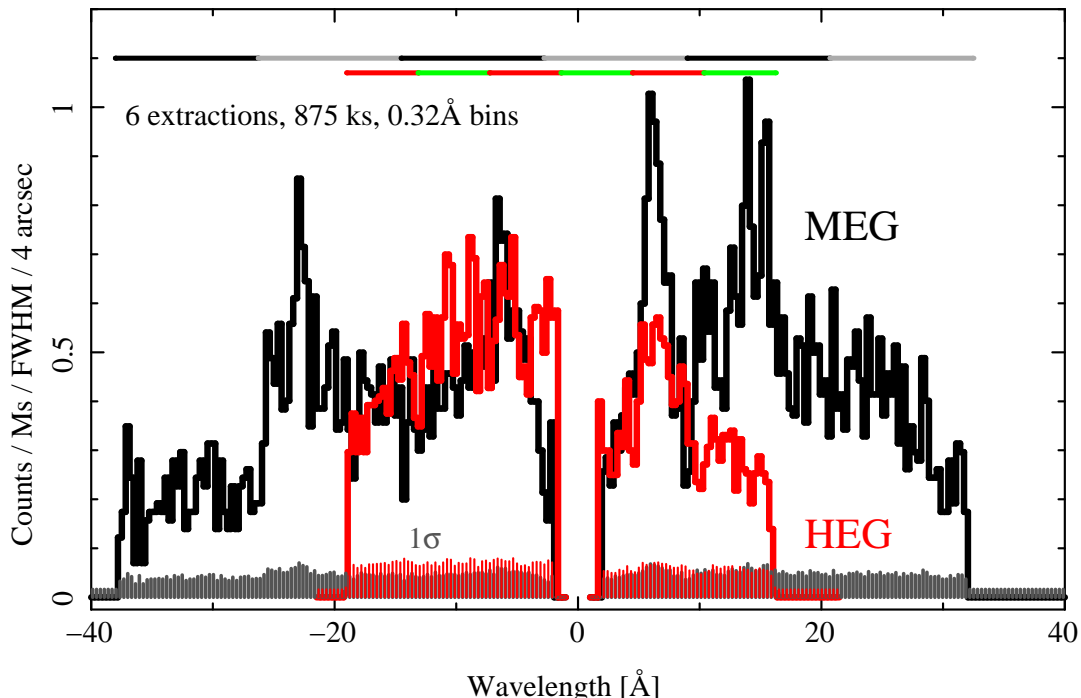
Figure 1 – The first orders' HETG count rate density, scaled to the FWHM in the dispersion direction and the default cross-dispersion extraction width for HEG (red) and MEG (black). The 1σ counting statistics uncertainty level is shown at the bottom of the plot. The approximate locations of each CCD are shown by the alternating color bars for MEG (upper) and HEG (lower), from S0 (leftmost, $CCD\_ID = 4$) to S5 ($CCD\_ID = 9$).

Table 1 – Observation Information

Target[a]	ObsID	Year	α[b] [deg]	δ[b] [deg]	l [deg]	b [deg]	T_{exp} [ks]
CH Cyg	1904	2001.24	291.16253	50.24519	81.8	+15.6	47
GS 1826-238[c]	6647	2006.61	277.10851	−23.79238	9.3	−6.1	159
GS 1826-238[c]	6647	2006.61	277.12700	−23.79130	9.3	−6.1	159
NGC 4388	9276	2008.30	186.45515	12.65497	279.1	+74.3	170
3C 445	13305	2011.59	335.96550	−2.09885	61.9	−46.7	163
NGC 3393	13967	2012.17	162.09595	−25.16997	270.7	+29.9	177

Table notes:

[a] The observer's intended target.

[b] The zeroth order position for the extracted spectrum, which is offset from the target and any visible sources in the field.

[c] Two extractions were done to obtain full coverage of HEG and MEG positive and negative orders, since the narrow sub-array does not give full coverage for any single zeroth order position.

2 Processing

We extracted spectra from the events using standard CIAO programs, but choosing a source position offset from the target position and from any other sources visible in the field. We did not use canonical "background regions" (adjacent to the source spectrum), but instead defined a wider source region for the spectral extraction to improve counting statistics. Two sets of rectangular regions are defined along each dispersion arm: mask regions are used to identify potential MEG and HEG events (the former taking precedence in areas where the masks overlap), and narrower extraction regions from which MEG and HEG events are extracted and binned into one-dimensional spectra. Custom spatial masks were narrower than defaults in order to lessen the extent of overlap near zeroth order and truncation of the spectra which otherwise occurs with a wider cross-dispersion spectral extraction width. Spatial mask full widths were $20.4\,\mathrm{arcsec}$ for both HEG and MEG (imaging focal length angle; $\simeq 41.5\,\mathrm{pixels}$). Cross-dispersion extraction full widths were $6.6 \times 10^{-3}\,\mathrm{deg}$ (or $\simeq 8.3\,\mathrm{pixels}$), which is about 5 times the default for point source extractions. We applied standard event grade and bad pixel filtering. Field images and spatial masks defining the spectral regions are shown in Appendix A.1.

3 Results

The count rate, scaled to the standard HEG and MEG extraction regions, is shown in Figure 1, and is below 1 count per bin per megasecond, where a bin is defined by the grating resolution FWHM ($23\,\mathrm{m\AA}$ for MEG and $12\,\mathrm{m\AA}$ for HEG), the default cross-dispersion extraction width ($1.32 \times 10^{-3}\,\mathrm{deg}$ in grating nodal angle, or $4.1\,\mathrm{arcsec}$ imaging angle), and the standard order-sorting region for $+1$ and -1 orders of MEG and HEG (about $500\,\mathrm{eV}$, but dependent on energy, CCD, and location, as defined by the `CALDB` "*OSIP*" file). An extraction cell for HEG or MEG is about $14.9\,\mathrm{pix}^2$, or $3.52\,\mathrm{arcsec}^2$.

We compared our measured HETG spectral rates to those that can be derived from the stowed background and found them to be similar. Hence, we conclude that the HETG backgrounds are primarily instrumental.

The observation which is near the galactic plane and at low galactic longitude (ObsID 6647), and might be expected to be higher due to any diffuse cosmic contribution, is higher in Figures 9 and 10, but comparable or higher rates are seen in another observation (ObsID 9276), which is far from the Galactic plane (see Table 1). While this has a relatively bright source in the field, estimates of source counts aliased by CCD readout into our background spectral region are comparable or less than the statistical uncertainty in our background count rate shown in Figure 1. We could not discern any significant difference in the HETG rate between observations, and so combined them all in Figure 1. The POG baseline rate (at wavelength extrema) are comparable to the median derived here.

If we examine the time-orderd rates for $CCD\_ID = 7$ ($S3$) (see Table 1 and Appendix A.3), the pattern mimics that of the background rates shown in the POG Figure 6.27, which is anti-correlated with solar activity, having high rates in 2008–2010.[2] Such events are likely high energy protons coming through the spacecraft.

For comparison to prior results, the Cycle 19 POG Figure 8.25 MEG rate value of $0.1\,\mathrm{counts/ks/\AA/6\,arcsec}$ near 10–$15\,\mathrm{\AA}$ corresponds to about a rate of $1.5\,\mathrm{counts/Ms/FWHM/4\,arcsec}$ in our scale on Figure 1, or 3 times larger than our current result.

---

[2]Also see `http://space.mit.edu/~cgrant/cti/cti120/bkg.pdf` for a graph of the "high energy reject rate" for S3.

4   Conclusions

The HETG background rate is less than $1.0\,\mathrm{counts/Ms/FWHM/4\,arcsec}$ (median value about 0.4) with about 10% uncertainty. This very low background rate is the result of two effects: the narrow spatial extraction regions possible with *Chandra*'s arcsecond resolution mirrors, and the order-sorting afforded by the energy resolution of the ACIS CCDs. That is, an event is only assigned to a grating spectrum if it is both at the right location with the right CCD PHA value.

Figure 2 shows the background rates as a flux, after applying the responses (by dividing the counts by exposure and the count rate for a constant spectrum of $1\,\mathrm{photons\,cm^{-2}\,s^{-1}\,keV^{-1}}$). This gives some indication of the flux limit due to the background.
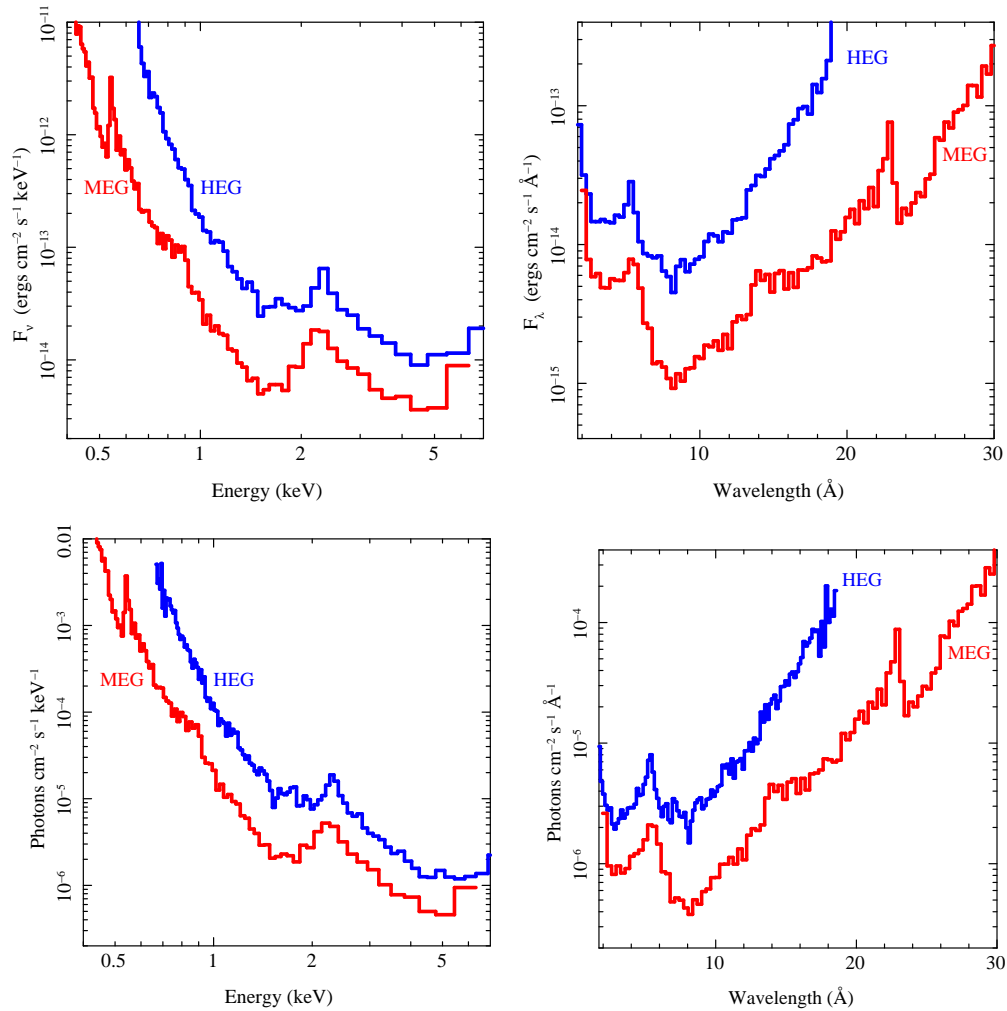
Figure 2 – The background count rate flux-corrected, as if from a cosmic source, vs energy (left) and wavelength (right), and for convenience, in photon units (bottom).

A   Additional Material

A.1   Field Images

Field images, showing the off-source extraction regions for each background spectral extraction. Note that the image aspect ratios are not square so chips are distorted into rectangles, and north and east vectors do not appear orthogonal.

Two independent extractions were done for ObsID 6647 (Figures 4 and 5) in order that extraction regions cover the entire range of CCDs, given the narrow sub-array.

Moderately bright sources are seen in Figures 6 and 7.

ObsID 13967 has a dropped S0 (CCD_ID 4), hence the blank are at the left side of Figure 8.
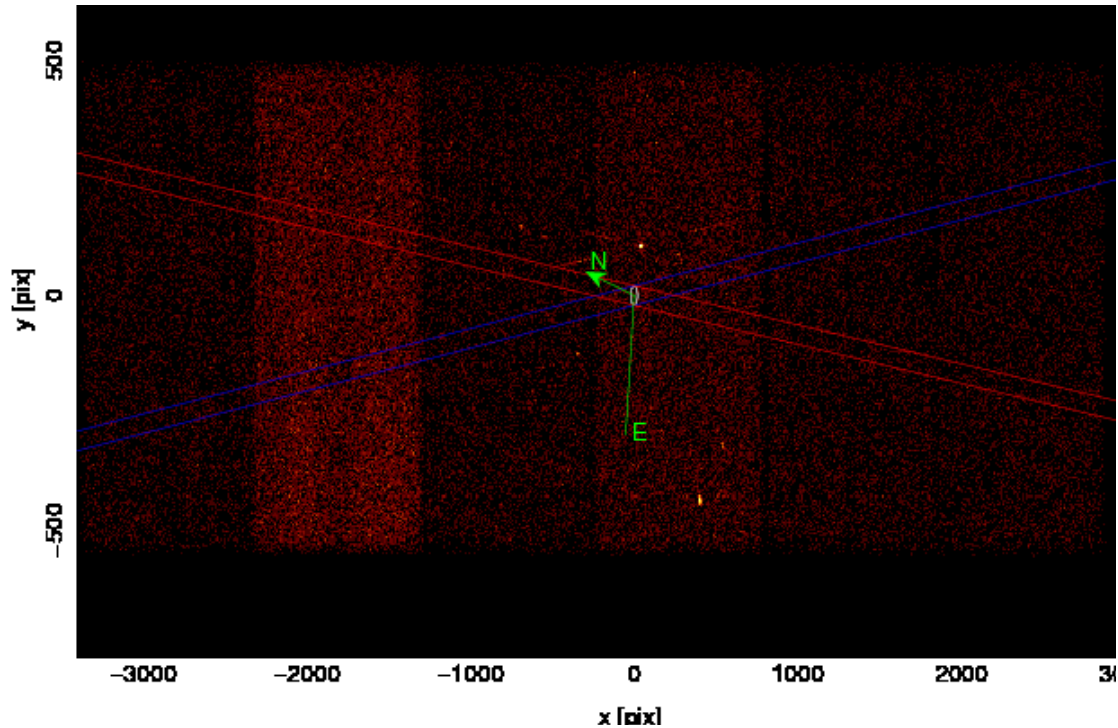
Figure 3 – ObsID 1904 Level 2 field image. The green circle (distorted by the aspect ratio) marks the adopted zeroth order position. The blue outline indicates the HEG spatial mask, and the red outline is the MEG mask. Green vectors indicate North and East.
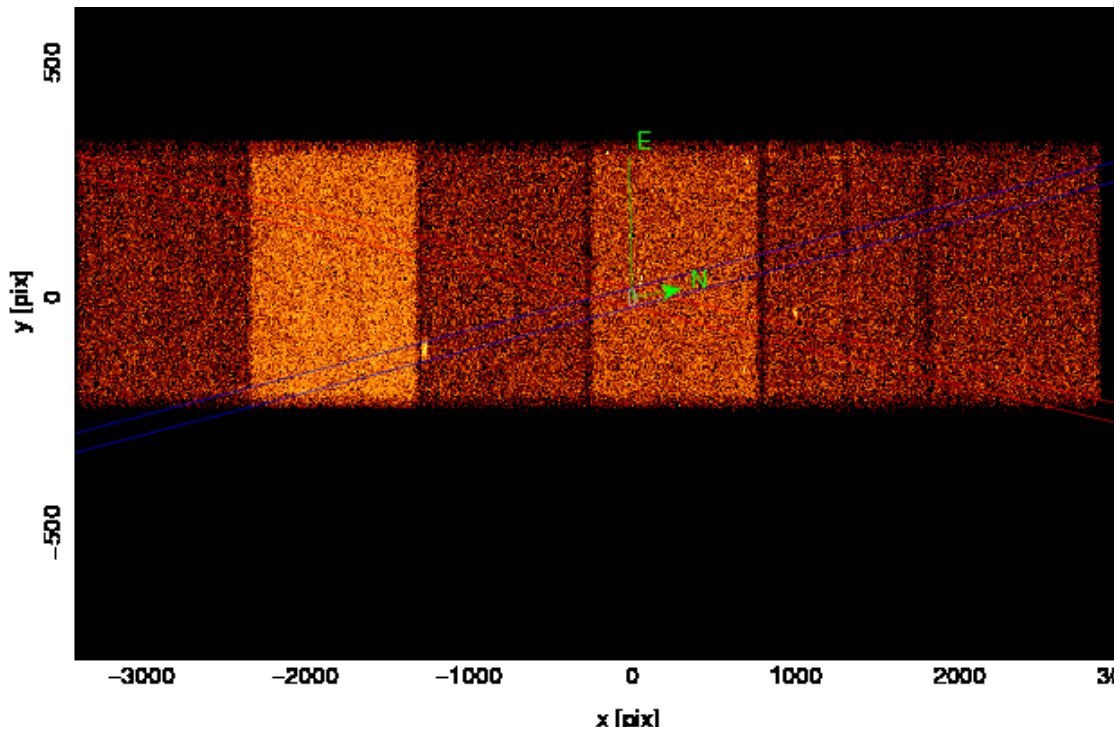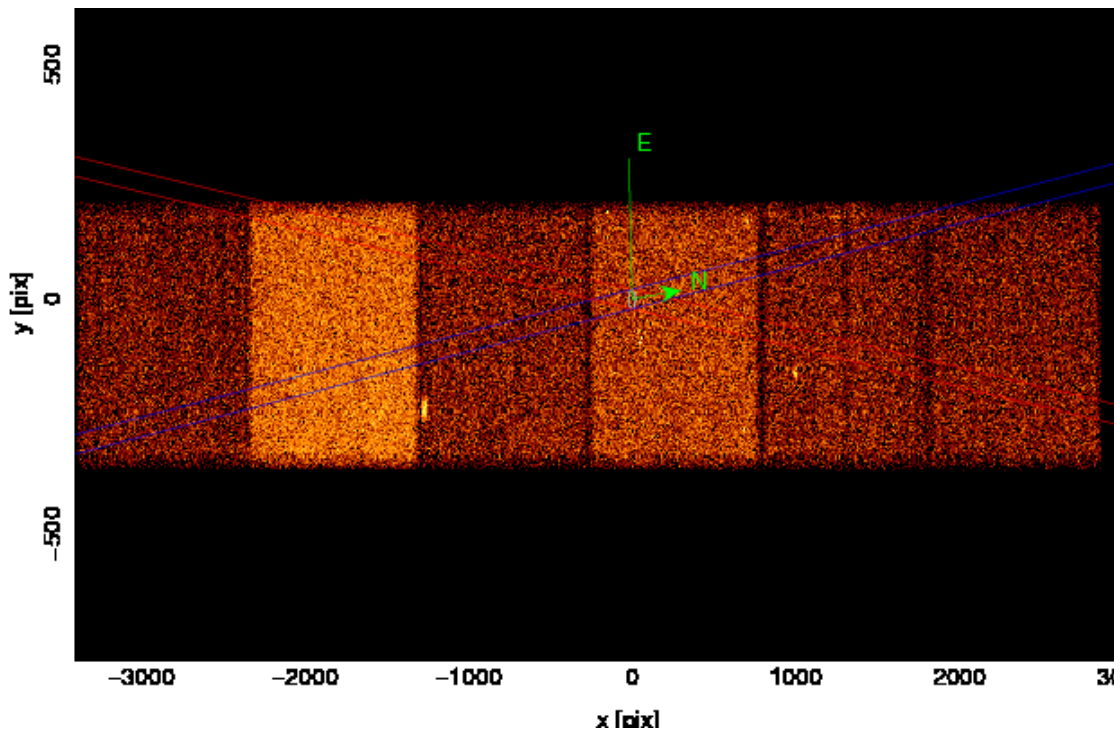
Figure 4 – ObsID 6647
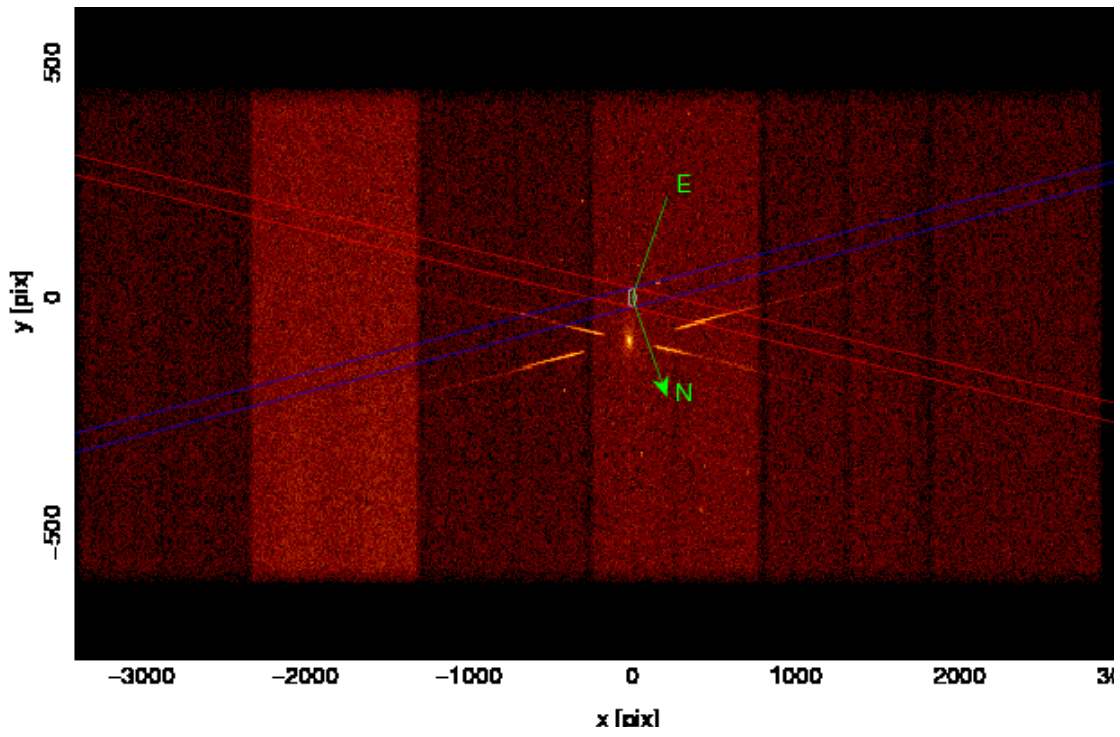

Figure 5 – ObsID 6647, second extraction.
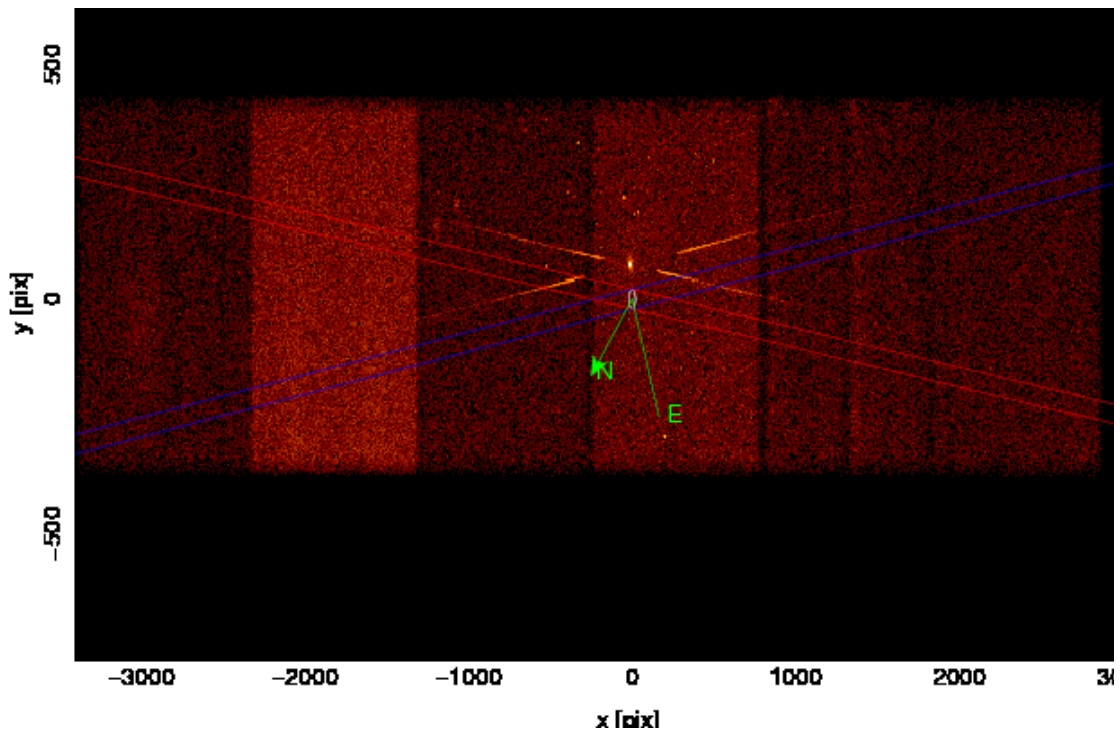
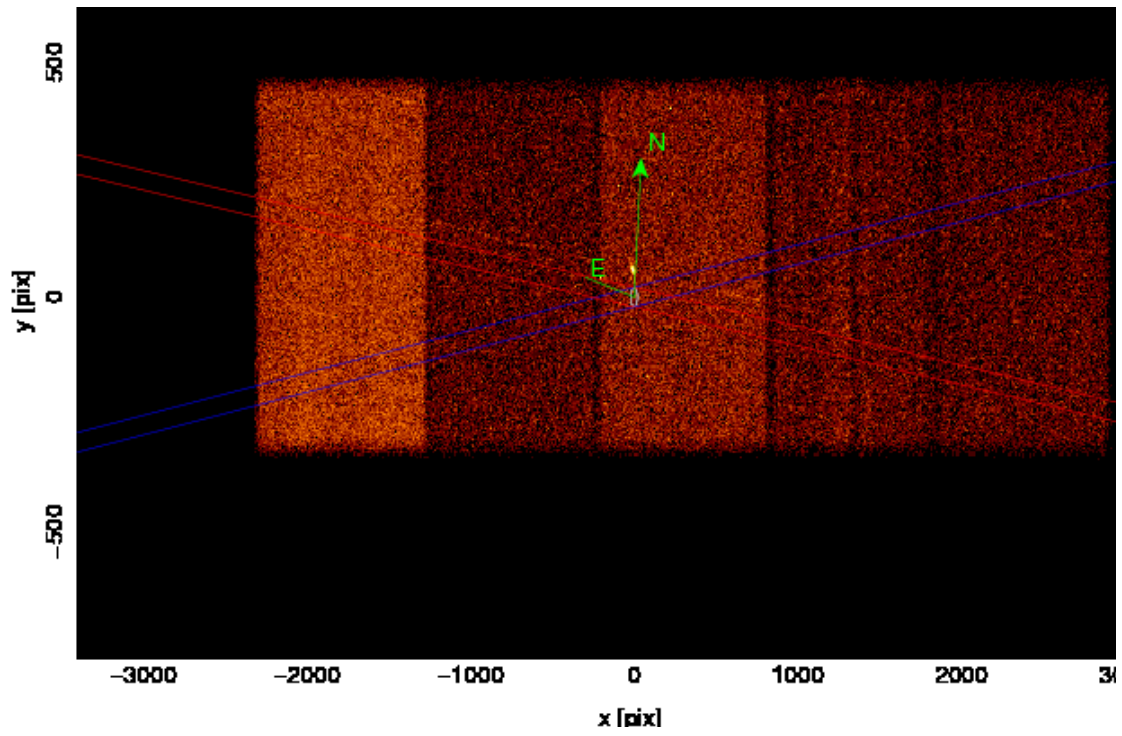**Figure 6** – ObsID 9276

Figure 7 – ObsID 13305

Figure 8 – ObsID 13967

A.2   CCD Resolution Spectra

For reference, Figure 9 shows the count rate spectra for each CCD and each observation from the level 2 event files (grade and status filtered). These include the source spectra, which accounts for some of the variance between ObsIDs, especially on $S2$ ($CCD\_ID = 6$) and $S3$ ($CCD\_ID = 7$)[3] where moderately bright sources are present (see Figures 6–7), though some of this is also apparently due to background fluctuations, since there are very few source counts on CCDs S0 and S5. The lines visible near $2\,\mathrm{keV}$ and near 8–$10\,\mathrm{keV}$ are instrumental, from particle induced fluorescence (see the *POG's* Figure 6.24). Some of the structure in Figure 1 is due to these features (e.g., near $7\,\text{Å}$).
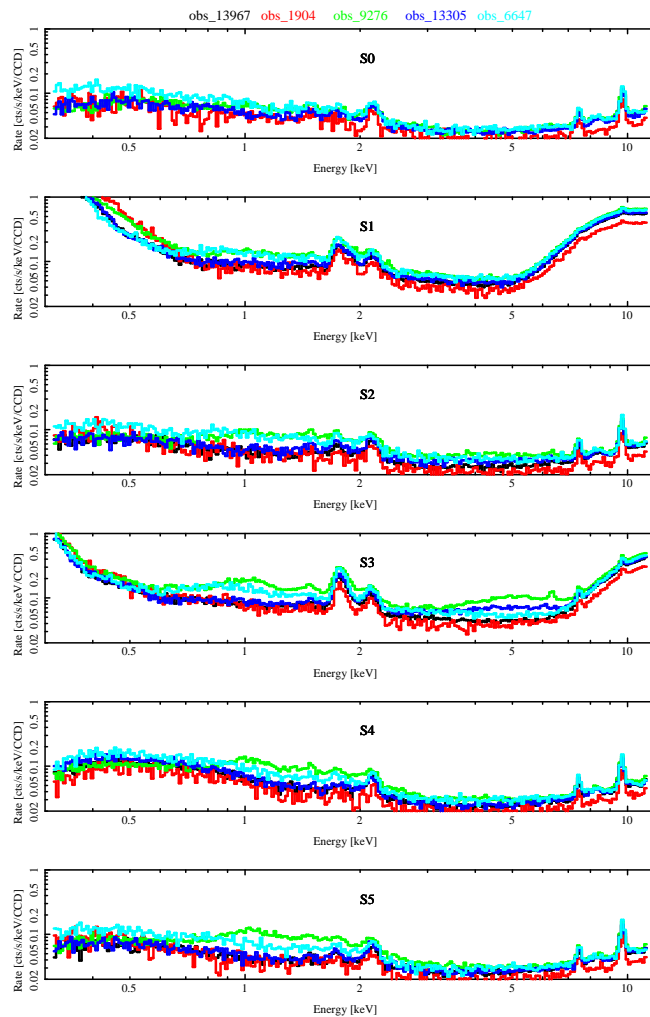

Figure 9 – PHA spectra for each CCD (S0 – S5, top to bottom panels) and each observation overplotted in each panel. Events were taken from the filtered (`evt2`) files. These spectra include the source events; rates have been scaled to a full 1024-row CCD. These rates are very similar to those shown in the *POG's* Figure 6.24.

---

[3]The 10 ACIS CCDs are enumerated with a CCD_ID running from 0–9, but also given enumerations on the imaging or spectroscopic arrays as $I0$–$I4$ and $S0$–$S5$.

A.3   CCD Count Rates

The rate per CCD between 0.4 and $7.0\,\mathrm{keV}$ is shown in Figure 10. These also include any sources in the field, but the energy region omits the large background tails at low and high energy which are not included in HEG or MEG spectra.
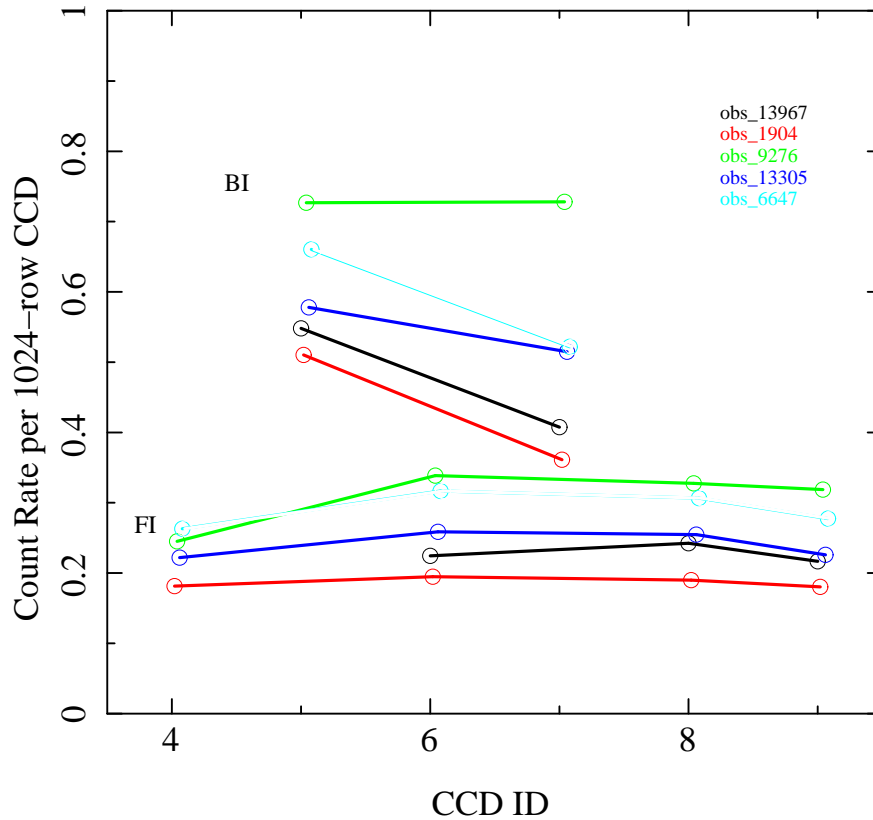

Figure 10 – CCD count rates for each observation, by `CCD_ID` and by object. Backside (BI) and fontside (FI) have been separated for clarity. If the observation used a sub-array, the rates were scaled to the full array equivalent. Events were taken from the filtered (`evt2`) files and further limited to CCD energies of 400–$7000\,\mathrm{eV}$ (based on the `ENERGY` column, which is scaled `PI` value, and not a model intrinsic energy). These rates include the source events.